

FERMIONIC ATOMS WITH TUNABLE INTERACTIONS IN  
A 3D OPTICAL LATTICE

T. STOFERLE, H. MORITZ, C. SCHORL, K. J. GUNTER, M. KOHL,  
T. ESSLINGER

Institute of Quantum Electronics,  
ETH Zurich Honggerberg,  
CH-8093 Zurich, Switzerland  
E-mail: stoeflerle@phys.ethz.ch

We report on the realization of a quantum degenerate atomic Fermi gas in an optical lattice. Fermi surfaces of noninteracting fermions are studied in a three-dimensional lattice. Using a Feshbach resonance, we observe a coupling of the Bloch bands in the strongly interacting regime.

## 1. Introduction

The exploration of quantum degenerate gases of fermionic atoms is driven by the ambition to gain deeper insight into long-standing problems of quantum many-body physics. So far, however, the analogy to an electron gas in a solid is limited since there the electrons experience a periodic lattice potential. The lattice structure is in fact a key ingredient for most models describing quantum many-body phenomena in materials. We access this regime by preparing a degenerate atomic Fermi gas in the crystal structure of an optical lattice.

In our experiment we load a noninteracting gas of  $^{40}\text{K}$  atoms into a three-dimensional optical lattice with simple cubic symmetry and directly image the Fermi surfaces. Gradual filling of the lattice transforms the system from a normal state into a band insulator. Previous experiments with far-detuned three-dimensional optical lattices were always carried out with bosonic atoms<sup>2;4;5</sup>, and experiments with fermions were restricted to a single standing wave<sup>6</sup>.

Interactions in the atomic Fermi gas can be tuned by using a Feshbach resonance between different spin components of the gas. By ramping the magnetic field into vicinity of the resonance, we increase the interactions between two particles residing on the same site of the lattice. In this manner

2

we dynamically induce a coupling between the lowest energy bands.

## 2. Preparing the degenerate Fermi gas in the 3D optical lattice

The apparatus and the procedure we use to create a degenerate atomic Fermi gas is described in previous work<sup>1</sup>. In brief, we use bosonic  $^{87}\text{Rb}$  to sympathetically cool a spin-polarized gas of fermionic  $^{40}\text{K}$  atoms to temperatures of  $T = 0.3 T_F$  ( $T_F = 260 \text{ nK}$  is the Fermi temperature of the noninteracting gas). The potassium atoms are then transferred from the magnetic trap into a crossed-beam optical dipole trap with a wavelength of  $\lambda = 826 \text{ nm}$ . There we prepare a spin mixture with (50 : 4)% in each of the  $|F = 9=2; m_F = -9=2\rangle$  and  $|F = 9=2; m_F = -7=2\rangle$  spin states using a sequence of two radio frequency pulses. After further evaporative cooling in the optical trap, we reach temperatures between  $T = 0.2 T_F$  and  $0.25 T_F$  with  $5 \cdot 10^4$  to  $2 \cdot 10^5$  particles, respectively.

Prior to loading the atoms into the optical lattice we tune the magnetic field to  $B = (210 \pm 0.1) \text{ G}$ , such that the s-wave scattering length between the two states vanishes. We exploit the magnetic Feshbach resonance between the  $|F = 9=2; m_F = -9=2\rangle$  and  $|F = 9=2; m_F = -7=2\rangle$  states<sup>7</sup> which is centered at  $B_0 = 202.1 \text{ G}$  and has a width of  $B = 7.8 \text{ G}$ . In this way we produce a two-component Fermi gas without interactions.

Then the standing wave laser field along the vertical z-axis is turned on. Subsequently, the optical dipole trap along the y-axis is turned on and a standing wave laser field along the same axis is turned on, followed by the same procedure along the x-axis. In order to keep the loading of the atoms into the lattice as adiabatic as possible, the intensities of the lasers are slowly increased (decreased) using exponential ramps with durations of 20 ms (50 ms) and time constants of 10 ms (25 ms), respectively. In its final configuration the optical lattice is formed by three orthogonal standing waves with a wavelength of  $\lambda = 826 \text{ nm}$ , mutually orthogonal polarizations and  $1/e^2$ -radii of 50  $\mu\text{m}$  (x-axis) and 70  $\mu\text{m}$  (y-axis and z-axis). The lattice depth  $V_0$  is calibrated by modulating the laser intensity and studying the parametric heating. The calibration error is estimated to be  $< 10\%$ .

## 3. Observing the Fermi surface

The potential created by the optical lattice results in a simple cubic crystal structure. The Gaussian intensity profiles of the lattice beams give rise to an additional confining potential which varies with the laser intensity. As

As a result, the sharp edges characterizing the  $T = 0$  distribution function for the quasimomentum in the homogeneous case are expected to be rounded off. Noninteracting fermions on a lattice with an additional harmonic confinement are described by the tight-binding Hamiltonian<sup>8</sup>

$$H = J \sum_{\langle i,j \rangle} \hat{c}_i^\dagger \hat{c}_j + \frac{m}{2} \sum_i (\omega_{\text{ext},x}^2 x_i^2 + \omega_{\text{ext},y}^2 y_i^2 + \omega_{\text{ext},z}^2 z_i^2) \hat{n}_i \quad (1)$$

Here  $\hat{c}_i^\dagger$  and  $\hat{c}_i$  denote the fermionic creation and annihilation operators for a particle at site  $i$ , and  $\hat{n}_i = \hat{c}_i^\dagger \hat{c}_i$  is the number occupation of site  $i$ . The first term with the tunneling matrix element  $J$  corresponds to the kinetic energy the particles gain through delocalization over the neighboring lattice sites. The second term accounts for a site-specific energy offset due to the harmonic confinement, which is represented by its trapping frequencies  $\omega_{\text{ext}}$  (with  $\omega_{\text{ext}} = x; y; z$ ). As the values of  $\omega_{\text{ext}}$  depend on the intensity of the lattice, changing the tunnel coupling  $J$  by varying the depth of the periodic potential results in a simultaneous change of the external confinement.

The harmonic confinement leads to a curvature of the Bloch bands in position space and, as a consequence, spatial regions with different fillings. For a given Fermi energy  $E_F$ , the filling in the center is highest and falls off to zero to the outer regions of the trap. When  $E_F$  exceeds the band width, a band insulating region appears first in the center of the trap, while regions farther out still have a filling below unity. However, due to the curved bands in position space, these atoms may still be spatially localized to a few lattice sites for small band widths<sup>3</sup>.

In the experiment we probe the population within the Brillouin zones by ramping down the optical lattice slowly enough for the atoms to stay adiabatically in the lowest band whilst quasimomentum is approximately conserved<sup>9</sup>. We lower the lattice potential to zero over a timescale of 1 ms. After an additional 1 ms we abruptly switch off the homogeneous magnetic field and allow for a total of 9 ms of ballistic expansion before we take an absorption image of the expanded atom cloud. The momentum distribution obtained from these time-of-flight images reproduces the quasimomentum distributions of the atoms inside the lattice.

With increasing particle number and confinement, the filling of the lattice sites increases. The initially circular shape of the Fermi surface (figure 1a) develops extensions pointing towards the Bragg planes (figure 1b) and finally transforms into a square shape completely filling the first Brillouin zone deeply in the band insulator. We have observed population of higher bands if more atoms are loaded into the lattice initially (figure 1c).

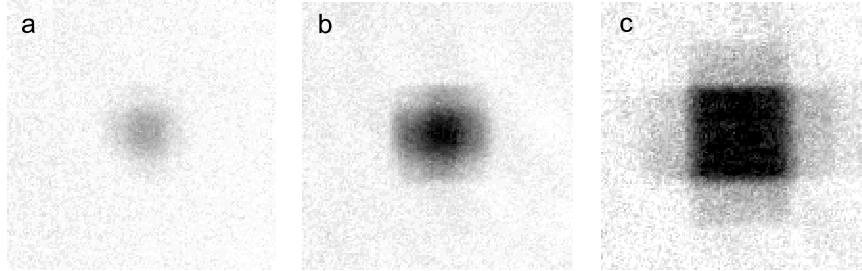


Figure 1. Development of the Fermi surface in quasimomentum space when more and more fermions are loaded into the lattice. a) 3500 atoms per spin state and  $V_0 = 5E_r$ . b) 15000 atoms per spin state and  $V_0 = 5E_r$ . c) 100000 atoms per spin state and  $V_0 = 20E_r$ . When the Fermi energy exceeds the initial width of the lowest Bloch band, higher Brillouin zones begin to become populated. As the band structure of the second and the third band in a 3D optical lattice overlap partially, both the second and the third Brillouin zone are being filled with atoms. Each of the three displayed quasimomentum distributions is obtained by averaging and smoothing 4 absorption images taken with the same parameters.

#### 4. Tuning the interactions

By using a Feshbach resonance, it is possible to tune continuously from attractive to repulsive s-wave interactions. When the on-site interaction is much smaller than the band gap, the physics in the lowest Bloch band can be described in the tight-binding approximation by a Hubbard Hamiltonian<sup>10</sup>. The phase diagram of the Fermi-Hubbard Hamiltonian is very rich, including Mott insulating<sup>11</sup> and antiferromagnetic phases<sup>12</sup>. We explore the limit where the wells of the lattice can be regarded as an array of isolated harmonic oscillator potentials, and we use a Feshbach resonance to tune the interactions between the particles in each of the wells.

In deep optical lattice potentials where tunneling is negligible, the Bloch bands are nearly flat and can be approximated by the levels of the harmonic oscillator inside each lattice well. When the s-wave interaction is changed on a time scale short compared to the tunneling time between adjacent potential minima, we may regard the band insulator as an array of more than ten thousand independent harmonic potential wells, each of which is populated by two particles. Solving the Schrodinger equation of two particles with a contact interaction in a harmonic oscillator yields<sup>13</sup>

$$\frac{a_s}{a_{ho}} = \frac{P - \frac{1}{2} (E = (2n!) + 3/4)}{(E = (2n!) + 1/4)} \quad (2)$$

where  $E$  denotes the eigenenergies for a given scattering length  $a_s$ , and  $n!$

is the trap frequency. The oscillator length  $a_{ho} = \sqrt{\frac{\hbar}{m \omega}}$  for a single lattice well in our system is on the order of  $1300 a_0$ . Figure 2a displays the energy spectrum as a function of the scattering length  $a_s$ .

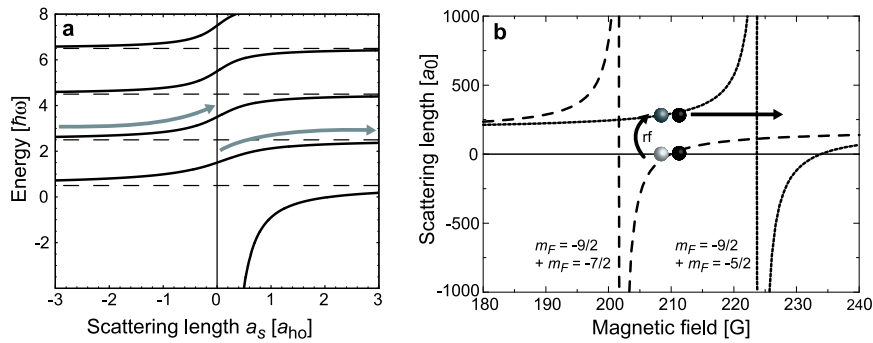


Figure 2. a) Energy spectrum of two strongly interacting particles in a three-dimensional harmonic oscillator potential which is given by equation (2) in the center-of-mass frame. The asymptotic energies at  $a_s \rightarrow \pm \infty$  are indicated by the dashed lines. The arrows show the direction of our sweep over the Feshbach resonance. b) Experimental method to observe interaction-induced transitions between Bloch bands. Two Feshbach resonances between the  $|F = 9=2; m_F = -9=2\rangle$  and  $|F = 9=2; m_F = -7=2\rangle$  states (dashed line, left) and the  $|F = 9=2; m_F = -9=2\rangle$  and  $|F = 9=2; m_F = -5=2\rangle$  states (dotted line, right) are exploited to tune the interactions in the gas. Using an rf pulse, we transfer the atoms from the  $|F = 9=2; m_F = -7=2\rangle$  to the  $|F = 9=2; m_F = -5=2\rangle$  state prior to sweeping over the Feshbach resonance at  $224.2 \text{ G}$ .

On the Feshbach resonance, the scattering length has a pole ( $a_s \rightarrow \pm \infty$ ). When sweeping adiabatically over the Feshbach resonance from magnetic fields below the resonance, we first increase the repulsive interaction between the two atoms in the oscillator ground state from the value of the background scattering length to  $a_s \rightarrow +\infty$  on the resonance. There the energy level of the lowest harmonic oscillator level becomes degenerate with the energy of the second next level, which is lowered from its noninteracting value because of the divergence  $a_s \rightarrow \pm \infty$  on the resonance. If projected onto the noninteracting eigenstates, this corresponds to a superposition of many higher oscillator states. When continuing the magnetic field sweep to values where the scattering length is again near zero, the atoms may adiabatically follow the higher oscillator level. This simple picture of two strongly interacting atoms in a well gives a qualitative understanding on what happens when atoms in a three-dimensional optical lattice cross a Fes-

Feshbach resonance: The higher energy bands get populated due to interaction induced coupling between the Bloch bands.

We experimentally investigate the interacting regime in the lattice starting from a noninteracting gas deep in a band insulator with  $V_x = 12 E_r$  and  $V_y = V_z = 18 E_r$  and corresponding trapping frequencies of  $\nu_x = 2 \times 50 \text{ kHz}$  and  $\nu_y = \nu_z = 2 \times 62 \text{ kHz}$  in the individual minima. A short radio-frequency pulse of 40 ns is applied to transfer all atoms from the  $|F = 9=2; m_F = -7=2\rangle$  into the  $|F = 9=2; m_F = -5=2\rangle$  state, with the atoms in the  $|F = 9=2; m_F = -9=2\rangle$  remaining unaffected. Then we ramp the magnetic field to different values around the Feshbach resonance<sup>14</sup> located at  $B_0 = 224.2 \text{ G}$  which has a width of  $\Delta B = 9.7 \text{ G}$ . The sweep approaches the Feshbach resonance from the side of repulsive interactions and crosses the resonant point where the scattering length diverges towards the side of attractive interactions, as depicted in figure 2b. When using this direction of the sweep there is no adiabatic conversion to molecules. After turning off the optical lattice adiabatically and switching off the magnetic field we measure the momentum distribution. To see the effect of the interactions we determine the fraction of atoms transferred into higher bands.

Figure 3a shows the measurement results when ramping the magnetic field to different values around the Feshbach resonance with a fixed inverse sweep rate of  $12 \text{ s/G}$ . For small magnetic field values well above the Feshbach resonance we observe a significant increase in the number of atoms in higher bands along the weak axis of the lattice, demonstrating an interaction induced coupling between the lowest bands. When we choose symmetrical lattice intensities, the atoms in the higher bands are distributed over all three dimensions since the oscillator levels are degenerate. By using a single, weaker axis we lift this degeneracy and transfer only to the higher bands along this direction, which increases our signal-to-noise ratio crucially.

Initially, one might expect that all atoms should be transferred to the higher bands. However, the process could be limited by the actual number of doubly occupied lattice sites which constitutes an upper bound for the transferred fraction. The inhomogeneous filling of the lattice and the finite temperature give rise to a significant amount of singly occupied sites, especially in the regions away from the center. When we vary the hold time at the small magnetic field far above the resonance, we do not observe a significant dependence on the measured fraction of atoms in the higher bands (figure 3b). Very recent theoretical studies<sup>15;16</sup> are beginning to shed light

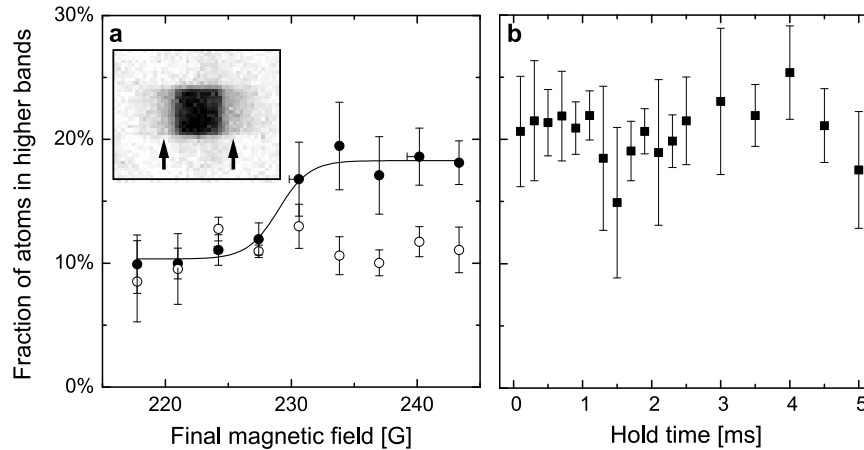


Figure 3. Interaction induced transition between Bloch bands. a) A fraction of the fermions is transferred into higher bands using a sweep across the Feshbach resonance (filled symbols). The line shows a sigmoidal fit to the data. The open symbols show a repetition of the experiment with the atoms prepared in the spin states  $|F = 9=2; m_F = 9=2 \rangle$  and  $|F = 9=2; m_F = 7=2 \rangle$  where the scattering length is not sensitive to the magnetic field. The magnetic field is calibrated by rf spectroscopy between Zeeman levels. Due to the rapid ramp the field lags behind its asymptotic value and the horizontal error bars represent this deviation. The data is taken from reference [1]. The inset shows the quasimomentum distribution for a final magnetic field of 233 G, for which the images of 4 measurements have been averaged and smoothed. Arrows indicate the atoms in the higher bands. b) Measured fraction in the higher bands versus the hold time at 233.8 G after the sweep. The vertical error bars show the statistical error of 4 repetitive measurements.

onto physics beyond the single-band description of the Feshbach resonance in the lattice.

## 5. Conclusions

In our experiments, we have realized a degenerate Fermi gas with tunable interactions in a three-dimensional optical lattice. We have demonstrated the control over parameters of the system such as filling and interactions. In the noninteracting, static regime, we image the shape of the Fermi surface for different characteristic densities. Our measurements in the strongly interacting regime where we observe a dynamical coupling of the Bloch bands pose challenges for the present theoretical understanding of many-particle fermionic systems in optical lattices. This very generic implementation of a fermionic many-particle quantum system on a lattice is expected to provide new avenues to intriguing phenomena of quantum many-body physics. The

unique control over all relevant parameters in this intrinsically pure system allows us to carry out experiments which are not feasible with solid-state systems.

Acknowledgments

We would like to thank SNF and QSIT for funding.

#### References

1. M. Kohl, H. Moritz, T. Stoferle, K. J. G. Günter, and T. Esslinger, *Phys. Rev. Lett.* **94**, 080403 (2005).
2. M. T. DePue, C. McCormick, S. L. Winoto, S. Oliver, and D. S. Weiss, *Phys. Rev. Lett.* **82**, 2262 (1999).
3. L. Pezze, L. Pitaevskii, A. Smerzi, S. Stringari, G. Modugno, E. de Mirandes, F. Ferlaino, H. Ott, G. Roati, and M. Inguscio, *Phys. Rev. Lett.* **93**, 120401 (2004).
4. M. Greiner, O. Mandel, T. Esslinger, T. W. Hansch, and I. Bloch, *Nature* **415**, 39 (2002).
5. T. Stoferle, H. Moritz, C. Schori, M. Kohl, and T. Esslinger, *Phys. Rev. Lett.* **92**, 130403 (2004).
6. G. Modugno, F. Ferlaino, R. Heidemann, G. Roati, and M. Inguscio, *Phys. Rev. A* **68**, 011601(R) (2003).
7. C. A. Regal, M. Greiner, and D. S. Jin, *Phys. Rev. Lett.* **92**, 083201 (2004).
8. M. Rigol and A. Muramatsu, *Phys. Rev. A* **70**, 043627 (2004).
9. M. Greiner, I. Bloch, O. Mandel, T. W. Hansch, and T. Esslinger, *Phys. Rev. Lett.* **87**, 160405 (2001).
10. D. Jaksch, C. Bruder, J. I. Cirac, C. W. Gardiner, and P. Zoller, *Phys. Rev. Lett.* **81**, 3108 (1998).
11. M. Rigol, A. Muramatsu, G. G. Batrouni, and R. T. Scalettar, *Phys. Rev. Lett.* **91**, 130403 (2003).
12. W. Hofstadter, J. I. Cirac, P. Zoller, E. Demler, and M. D. Lukin, *Phys. Rev. Lett.* **89**, 220407 (2002).
13. T. Busch, B.-G. Englert, K. Rzazewski, and M. Wilkens, *Found. Phys.* **28**, 549 (1998).
14. C. A. Regal and D. S. Jin, *Phys. Rev. Lett.* **90**, 230404 (2003).
15. D. B. M. Dickerscheid, U. AlKhawaja, D. van Oosten, and H. T. C. Stoof, *Phys. Rev. A* **71**, 043604 (2005).
16. R. B. Diener and T.-L. Ho, *arXiv e-print, cond-mat/0507253*.